Metformin confers longitudinal cardiac protection by preserving mitochondrial homeostasis following myocardial ischemia/reperfusion injury

Jing Tian (tianjing-med@hotmail.com)
Beijing An Zhen Hospital: Capital Medical University Affiliated Anzhen Hospital

Yaqi Zheng
Beijing An Zhen Hospital: Capital Medical University Affiliated Anzhen Hospital

Tiantian Mou
Beijing An Zhen Hospital: Capital Medical University Affiliated Anzhen Hospital

Mingkai Yun
Beijing An Zhen Hospital: Capital Medical University Affiliated Anzhen Hospital

Yi Tian
Beijing An Zhen Hospital: Capital Medical University Affiliated Anzhen Hospital

Yao Lu
Beijing An Zhen Hospital: Capital Medical University Affiliated Anzhen Hospital

Yujie Bai
Beijing An Zhen Hospital: Capital Medical University Affiliated Anzhen Hospital

Yihan Zhou
Beijing An Zhen Hospital: Capital Medical University Affiliated Anzhen Hospital

Marcus Hacker
Medical University of Vienna Department of Biomedical Imaging and Image-guided Therapy: Medizinische Universitat Wien Universitatsklinik fur Radiologie und Nuklearmedizin

Xiaoli Zhang
Beijing An Zhen Hospital: Capital Medical University Affiliated Anzhen Hospital https://orcid.org/0000-0002-0770-5594

Xiang Li
Medical University of Vienna Department of Biomedical Imaging and Image-guided Therapy: Medizinische Universitat Wien Universitatsklinik fur Radiologie und Nuklearmedizin

---

Research Article

Keywords: Myocardial I/R injury, TSPO, mitochondrial homeostasis, metformin, spatio-temporal effect

Posted Date: April 13th, 2022

DOI: https://doi.org/10.21203/rs.3.rs-1502437/v1

Abstract

Purpose

Myocardial ischemia-reperfusion (I/R) injury is associated with systemic oxidative stress, cardiac mitochondrial homeostasis, and cardiomyocyte apoptosis. Metformin was recognized to attenuate cardiomyocyte apoptosis. However, the longitudinal effects and pathomechanism of metformin on the regulation of myocardial mitohormesis following I/R treatment remain unclear. The aim of this study was to investigate the longitudinal effects and mechanism of metformin in regulating cardiac mitochondrial homeostasis by serial imaging with the 18-kDa translocator protein (TSPO)-targeted positron emission tomography (PET) tracer ^{18}F-FDPA.

Methods

Myocardial I/R injury was established in Sprague-Dawley rats, which were treated with or without metformin (150 mg/kg per day). Serial gated ^{18}F-FDG and ^{18}F-FDPA PET imaging were performed at 1, 4, and 8 weeks after surgery, followed by analysis of ventricular remodelling and cardiac mitochondrial homeostasis. After PET imaging, the activity of antioxidant enzymes, immunostaining, and western blot analysis were performed to analyse the spatio-temporal effects and pathomechanism of metformin for cardiac protection after myocardial I/R injury.

Results

Oxidative stress and apoptosis increased one week after myocardial I/R injury (before significant progression of ventricular remodelling). TSPO co-localized with inflammatory CD68$^+$ macrophages in the infarct area, and upregulation of AMPK-p/AMPK and down-regulation of Bcl-2/Bax were observed. However, these effects were reversed with metformin treatment. Eight weeks after myocardial I/R injury (representing the advanced stage of heart failure), ^{18}F-FDPA uptake activity in myocardial cells in the distal non-infarct area increased without CD68$^+$ expression, whereas the activity decreased with metformin treatment.

Conclusion

Taken together, these results show that prolonged metformin treatment has pleiotropic protective effects against myocardial I/R injury associated with a regional and temporal dynamic balance between mitochondrial homeostasis and cardiac outcome, which were assessed by TSPO-targeted imaging during cardiac remodelling.

Introduction

Myocardial ischemia-reperfusion (I/R) injury causes severe manifestations, including left ventricular remodelling and cardiac dysfunction, which ultimately exacerbate, leading to heart failure [1, 2]. Oxidative metabolism in the mitochondria is the main source of cardiac energy consumption, and mitochondrial dysfunction is considered the primary mechanism linking cardiac contractile failure after myocardial I/R injury [3]. The mammalian mitochondrial permeability transition pore (mPTP) is essential for maintaining mitochondrial homeostasis and membrane potential [4]. The irreversible myocardial damage following myocardial I/R injury has been proposed to involve mPTP opening. Thus, myocardial I/R injury appears to be closely linked to mitochondrial impairment. Moreover, excessive production of reactive oxygen species (ROS) is involved in several detrimental processes, including cell apoptosis triggered by opening of the mPTP [5]. Indeed, enhanced ROS production is related to microvascular pathologies under myocardial ischemia conditions. Excessive ROS generally causes an inflammatory response by disrupting mitochondrial membrane homeostasis [6]. Therefore, therapeutic strategies for I/R injury have been developed targeting mPTP inhibition to modulate energy homeostasis, mitochondrial function, and ROS production in cardiomyocytes.

One such strategy may involve the repurposing of metformin, which is widely used to treat type 2 diabetes and also has a cardiac-protective mechanism that is proposed to be related to the mitochondria-mediated modulation of energy homeostasis. Metformin was reported to activate AMP-activated protein kinase (AMPK), an intracellular energy sensor in intact cardiomyocytes [7, 8]. Several studies corroborated that metformin may regulate mitochondrial homeostasis by restoring myocardial AMPK and reducing oxidative stress [9, 10]. However, the underlying mechanism and longitudinal cardio-protection effects of metformin in association with mitohormesis have not been clearly elucidated.

There is increasing recognition of the need for specific diagnostic biomarkers of myocardial I/R injury that can accurately assess myocardial death progression from a stress injury. Translocator protein (TSPO) is an 18-kDa protein that is a key component of the mPTP and plays an essential role in regulating innate immunity [11]. TSPO is mainly expressed on the mitochondrial membrane [12], which is involved in the pathophysiological processes of mitochondrial homeostasis, apoptosis, and oxidative stress. In addition, upregulation of TSPO expression was found to be associated with the accumulation of ROS and the breakdown of mitochondrial homeostasis. Combined with such markers, advances in molecular imaging are expected to help identify myocardial I/R injury and facilitate timely intervention with effective therapies to prevent cardiac deterioration. Fluorine-18–labelled N,N-diethyl-2-(2-(4-(2-fluoroethoxy)phenyl)-5,7-dimethylpyrazolo[1,5-a]pyrimidin-3-yl)acetamide (^{18}F-FDPA) was developed as a novel TSPO-specific radioligand, which can be used to detect activated microglia in neurodegenerative disorders [13, 14]. Our previous study [15] indicated that the increased cardiac uptake of ^{18}F-FDPA in rats with acute myocardial infarction at one week after surgery was related to the infiltration of inflammatory cells. Nevertheless, the utility of ^{18}F-FDPA in TSPO imaging for quantification of the degree of cardiac mitochondrial homeostasis after myocardial I/R injury has not been assessed.

Accordingly, the primary aim of the present study was to investigate the spatio-temporal effects and pathomechanism of metformin for cardiac protection after myocardial I/R injury. Specifically, we serially

evaluated *in vivo* myocardial TSPO expression in correlation with the extent of mitochondrial homeostasis and cardiac function in a rat model of myocardial I/R injury using ^{18}F-FDPA positron emission tomography (PET) imaging.

Material And Methods

Animal model

Thirty-six male Sprague–Dawley rats (280–300 g) were purchased from SPF Biotechnology Co., Ltd. (Beijing, China) and underwent transient coronary artery ligation to induce myocardial I/R or sham surgery as previously described [16, 17]. In brief, the rats were anaesthetised with soflurane (4.0% induction, 2.0% maintenance) and mechanically ventilated with a tidal volume of 8.0–13.0 ml/kg, a respiratory rate of 80 breaths per minute, and an inspiratory-to-expiratory ratio of 1:2. A 7 − 0 polypropylene suture with a curved needle was placed under the origin of the left anterior descending (LAD) artery and a medical latex tube was placed over the artery. Myocardial ischemia was induced by tightening the suture for 30 min. Successful induction of myocardial ischemia was verified by the presence of ST-segment elevation on electrocardiography. The suture was then loosened to restore coronary circulation, ensuring that the myocardium turned grey after LAD ligation. Twenty-four rats with I/R were randomly divided into two groups: the vehicle (0.9% saline) group and metformin groups. The rats in the metformin group received metformin (150 mg/kg per day) every day for 8 weeks based on previous experiments [18, 19]. The other 12 rats were selected as the sham group. Sham-operated animals underwent the same surgical procedures but were not subjected to LAD coronary artery ligation. The experimental protocols are schematically displayed in Fig. 1.

According to the scheduled time point, animals were euthanized with an overdose of isoflurane (5.0% isoflurane with 2.0 L/min oxygen) followed by cervical dislocation. All animal experiments were performed according to Beijing's laboratory animal management regulations, and were approved by the Animal Care Committee of Capital Medical University (Ethical approval number: AEEI-2019-167).

Radiochemistry

^{18}F-FDPA was automatedly synthesized by the CFN-MPS200 module (Sumitomo Heavy Industries, Ltd., Tokyo, Japan), as described previously [15]. The radiochemical purity was > 99%. The molar activity was 273–532 GBq/μmol.

Whole-body small-animal PET/computed tomography (CT)

PET/CT imaging was performed with a dedicated micro-PET/CT scanner (Inveon PET/CT, Siemens, Germany). The rat was placed into a chamber connected to an isoflurane anaesthesia unit, and anaesthesia was induced using an airflow rate of 2.0 L/min containing 4.0% isoflurane. The animal was then immediately placed in a prone position on the scanning bed and the airflow rate was reduced to 0.8–1.5 L/min with 2–2.5% isoflurane. Approximately 74 MBq ^{13}N-NH_3 was injected via the tail vein, and

a dynamic 15-min (2 frames: 1 × 300 s, 1 × 600 s) image was acquired in list mode followed by a 2-beds CT scan using the “magnification low” acquisition setting (projection: 180; binning: 4 × 4; transaxial field of view: 53.9 mm; axial scanning length: 134 mm; voltage: 80 kV; current: 500 μA). Four hours after ^{13}N-NH_3 image acquirement, 29.6–33.3 MBq ^{18}F-FDG was injected via the tail vein. Forty minutes later, a 30-min gated PET scan was performed, followed by a CT scan following the same method described above. The next day, ^{18}F-FDPA (30.0–35.0 MBq) was injected into the same rat and a static 15-min PET image was acquired at 40 min post injection, followed by a CT scan according to the same method described above.

Image analysis

Images were analysed by two experienced nuclear cardiologists independently using Inveon Research Workplace software (Siemens) and the cardiac PMOD software 4.2 package (PMOD Technologies Ltd., Zurich, Switzerland). Heart analysis was performed as described previously [13, 20–22].

^{13}N-NH_3 perfusion imaging was assessed using an AHA 17-segment model according to the American Society of Nuclear Cardiology guidelines [23]. Each segment accounts for 6% of the left ventricle (LV). The total perfusion defect (TPD; percentage of the LV myocardium) was defined using a threshold (< 60%) of the normalized maximum signal of ^{13}N-NH_3 uptake [23, 24].

For quantification of ^{18}F-FDPA uptake in the whole myocardium, myocardium in the infarct territory, and remote non-infarct territory of the inferior wall, regions of interest (ROIs) in the ^{13}N-NH_3 polar maps were delineated and copied to the ^{18}F-FDPA polar maps to allow for precise, spatially matched quantification of ^{18}F-FDPA activity. To account for differences in tracer delivery, the regional or global mean standardized uptake value (SUVmean) of ^{18}F-FDPA in the LV and that in the left atrium (LA) were analysed. The global target-to-background ratio (TBR) in the whole heart was calculated as the global SUVmean/LA SUVmean, whereas the regional TBR was calculated as the regional SUVmean/LA SUVmean.

To assess myocardial systolic and diastolic function, electrocardiogram-gated ^{18}F-FDG was conducted serially at 1 week, 4 weeks, and 8 weeks post-I/R injury. The cardiac PMOD software was used to quantitatively measure the LV end-diastolic volume (LVEDV), end-systolic volume (LVESV), and LV ejection fraction (LVEF).

Histological analysis

Adjacent tissue sections were processed for histopathology as described previously [25]. Haematoxylin and eosin staining was used to define the general myocardial morphology. Leukocyte infiltration was identified by immunostaining CD68-positive macrophages using streptavidin horseradish peroxidase-diaminobenzidine visualization. For cellular differentiation, fluorescence immunostaining was conducted on inflammation-positive sections using CD68 rabbit polyclonal (GB113109, Servicebio) and rabbit anti-TSPO (NBP1-45769, Novus Biologicals), with DAPI staining of nuclei. The secondary antibody used for

CD68 and TSPO immunostaining were HRP-conjugated goat anti-rabbit IgG (H + L) (GB23303, Servicebio) and Cy3-conjugated goat anti-rabbit IgG (H + L) (GB21303, Servicebio), respectively.

Oxidative stress measurement

The concentrations of superoxide dismutase (SOD), malondialdehyde (MDA), and glutathione peroxidase (GSH-Px) in the rat serum were measured using corresponding enzyme-linked immunosorbent assay kits from Beijing Sinouk Institute of Biological Technology (Beijing, China) according to the manufacturer's protocols.

Western blot analysis

Western blot analysis was performed as described previously [26]. In brief, the protein concentration was measured using a bicinchoninic acid protein assay kit (YTHXBio, China). The extracted proteins were then separated by electrophoresis using a 12% sodium dodecyl sulphate polyacrylamide gel. The proteins were transferred to polyvinylidene fluoride membranes (Millipore, USA) and blocked using Tris-buffered saline with Tween buffer containing 3% BSA. The membranes were incubated with primary antibodies against Bax (1:500), phosphorylated AMPK (Thr 172) (1:1000), total AMPK (1:5000) (all from Cell Signaling Technology, Danvers, MA, USA), Bcl-2 (1:5000; Abcam), and GADPH (1:10000; YTHXBio, China) at 4°C overnight. The membranes were washed three times and then incubated with the horseradish peroxidase-conjugated secondary antibody (1:10,000) at 37°C for 40min. Finally, the bands were detected by an enhanced chemiluminescence kit (Millipore, USA) and the results were quantified using Total Lab Quant V11.5 (Newcastle upon Tyne, UK). The levels of Bcl-2/Bax (anti-/pro-apoptotic) proteins and AMPK-p/AMPK proteins were also normalized to that of GAPDH.

Statistical analysis

Data with a normal distribution are expressed as the mean ± standard deviation, whereas non-normally distributed data are expressed as the median and interquartile range. The mean values of continuous variables were compared between two groups using Student's t-test with normality or the Mann-Whitney *U* test without normality. Multiple groups were compared by analysis of variance followed by post-hoc testing with normality (Tukey's post-hoc tests with equal variance assumed or Dunnett's T3 test without equal variance assumed) or the Kruskal-Wallis H test without normality. $P < 0.05$ was defined as statistically significant. All statistical analyses were performed using SPSS software, version 26.0 (SPSS Inc., Chicago, IL, USA) and Prism 7 software (GraphPad).

Results

Metformin improved LV structure and function after myocardial I/R injury

Serial ^{13}N-NH_3 perfusion showed that the extent of TPD in the vehicle group exhibited a 10% decrease in the LV at 1 week after I/R injury (Fig. 2a). There was no significant difference in the TPD between the

vehicle group and metformin group over 8 weeks (Fig. 2a).

Functional analysis by serial gated ^{18}F-FDG PET/CT revealed no significant changes in the LVEF in the sham group over 8 weeks (Fig. 2d). After I/R injury, the rats in both the vehicle and metformin groups exhibited marked LV remodelling during follow-up, as attested by significant increases in the LVESV (Fig. 2c) and significant decreases in the LVEF (Fig. 2d) compared with those of the sham group. Notably, the LVEF in the metformin group was higher than that in the vehicle group and approached the normal level at 8 weeks, although the difference was not statistically significant, suggesting that the mechanisms underlying the response to metformin therapy are largely related to LV systolic function.

Metformin prevented oxidative stress and maintained mitochondrial homeostasis in rats after I/R injury during heart failure progression

After I/R injury, the metformin group exhibited an anti-oxidative stress response during follow-up, as attested by significant increases in the SOD and GSH-Px levels (all $P < 0.01$) (Fig. 3a,c), and decreases in the MDA level (all $P < 0.05$) (Fig. 3b) compared with those of the vehicle group.

The normalized SUV ratios of global cardiac ^{18}F-FDPA uptake to the LA (global TBR) in the vehicle group were markedly elevated at 4 weeks and 8 weeks compared with those of the sham group (all $P < 0.01$) (Figs. 4a and 5a), respectively. The TBR in the infarct territory was significantly lower than that in the remote territory at 1, 4, and 8 weeks after I/R injury (all $P < 0.01$) (Fig. 4b,c). Thus, this semi-quantitative analysis demonstrated that TSPO was overexpressed in the remote non-infarct territory of the myocardium rather than in the infarct territory of the myocardium in a time-dependent manner.

After I/R injury, the metformin group showed a significant decline in the TBRs of the global, infarct territory, and remote territory portions of the myocardium at 8 weeks compared with those of the vehicle group (Fig. 5a–d).

Metformin has temporal and regional protective effects after myocardial I/R injury

Effects of metformin on the infarct territory at 1 week after I/R injury

Haematoxylin and eosin staining showed massive accumulation of inflammatory cells in the infarct territory in the vehicle group at 1 week after I/R injury (Fig. 6a, i). Immunofluorescence confirmed that the elevated TSPO signal in the infarct territory co-localised with abundant CD68^{+} inflammatory cells in both the vehicle and metformin groups (Fig. 6b, iii). To assess the presence of regional cell survival and the AMPK-dependent regulatory pathway in mitochondrial homeostasis, we evaluated the relative protein expression levels of Bcl-2/Bax and AMPK-p/AMPK by western blot analysis. The levels of Bcl-2/Bax in the vehicle group exhibited an 89% ($P = 0.001$) decrease compared with those of the sham group in the infarct territory at 1 week after I/R injury. However, this decrease in the levels of Bcl-2/Bax was prevented

in the metformin group (Fig. 6c). Notably, the levels of AMPK-p/AMPK in the vehicle group showed a 6-fold increase ($P = 0.001$) compared with those of the sham group. Nevertheless, this increase in the levels of AMPK-p/AMPK was abrogated in the metformin group (Fig. 6e). These results suggested that metformin protects against I/R-induced apoptosis by inhibiting endogenous AMPK in the infarct territory at the acute phase.

Effects of metformin on the remote non-infarct territory at 1 week after I/R injury

Without $CD68^+$ co-localisation, TSPO staining was consistent with the presence of non-inflammatory cells in the remote non-infarct territory at 1 week after I/R injury (Fig. 6a,b; ii). In parallel, the increase in the TSPO signal was reduced with metformin treatment (Fig. 6a,b; iv). Western blot analysis showed that the levels of Bcl-2/Bax in the vehicle group were 84% ($P < 0.001$) lower than those in the sham group in the remote non-infarct territory at 1 week after I/R injury, and this decrease was prevented in the metformin group (Fig. 6d). However, there was no significant difference in the levels of AMPK-p/AMPK between the vehicle and metformin groups (Fig. 6f).

Effects of metformin on the infarct territory at 8 weeks after I/R injury

Without $CD68^+$ co-localisation, TSPO staining was consistent with non-inflammatory cells in the infarct territory at 8 weeks after I/R injury (Fig. 7a,b; i). In parallel, the increase in the TSPO signal was reduced with metformin treatment (Fig. 7a,b; iii). Western blot analysis showed that the levels of Bcl-2/Bax in the vehicle group were 73% ($P < 0.001$) lower than those in the sham group in the infarct territory at 8 weeks after I/R injury. However, this decrease in Bcl-2/Bax levels was prevented in the metformin group (Fig. 7c). There was no significant difference in the levels of AMPK-p/AMPK between the vehicle and metformin groups (Fig. 7e).

Effects of metformin on the remote non-infarct territory at 8 weeks after I/R injury

Without $CD68^+$ co-localisation, TSPO staining was consistent with the non-inflammatory cells in the remote non-infarct territory at 8 weeks after I/R injury (Fig. 7a,b; ii). In parallel, the increase in the TSPO signal was lower with metformin treatment (Fig. 7a,b; iv). Western blot analysis showed that the levels of Bcl-2/Bax in the vehicle group were 35% ($P = 0.028$) lower than those in the I/R + sham group in the remote non-infarct territory at 8 weeks after I/R injury. A significant increase in the Bcl-2/Bax ratio was observed in the metformin group as compared with that of the vehicle group (Fig. 7d). The AMPK-p/AMPK ratio in the vehicle group exhibited a 93% ($P < 0.001$) decrease compared with that in the sham group, consistent with the pattern for Bcl-2/Bax expression. However, this decrease in the AMPK-p/AMPK ratio was prevented in the metformin group (Fig. 7f). Thus, metformin protected against I/R-induced apoptosis by promoting exogenous AMPK in the remote territory at the chronic phase.

Discussion

Severe and extensive myocardial injury leads to cellular metabolic disorder, in which the synthesis of mitochondrial ATP in the respiratory chain is reduced and ROS excessively accumulate, thus increasing the opening of the mPTP, leading to irreversible depolarisation of mitochondrial membrane potential, causing the imbalance of myocardial mitochondrial homeostasis, eventually resulting in cell death [27]. Consistently, in this study, we found that with aggravation of the myocardial I/R-induced damage response, the levels of SOD and GSH-Px in the blood gradually decreased, the content of MDA gradually increased, and the *in vivo* TSPO expression in the whole heart gradually increased. The results suggested that the extent of generation of ROS and mitochondrial homeostasis imbalance were time-dependent and related to the severity of myocardial I/R injury. Metformin is a drug used for the clinical treatment of diabetes, which can activate AMPK by increasing the AMP/ATP ratio in cells and up-regulates the antioxidant enzyme SOD to reduce myocardial I/R injury [28]. After intervention with metformin, with the prolongation of treatment time, the serum SOD and GSH-Px levels of the rats gradually increased, and the MDA content gradually decreased. The ^{18}F-FDPA uptake activity in the global heart *in vivo* PET imaging was reduced. Taken together, these results indicated that metformin could enhance the activity of antioxidant enzymes and maintain myocardial mitochondrial homeostasis after I/R injury.

Endogenous AMPK activation and mitochondrial homeostasis imbalance are important factors in promoting apoptosis in myocardial I/R injury [29, 30]. Previous studies demonstrated that under stress conditions, the macrophage migration inhibitory factor (MIF) up-regulates and activates a variety of receptors on macrophages [31] [32], and eventually causes myocardial cell apoptosis. In this study, at one week after myocardial I/R injury, AMPK-p/AMPK protein expression was up-regulated, whereas Bcl-2/Bax protein expression was down-regulated, and TSPO and CD68$^+$ (a macrophage marker) co-localised in the infarct area with high expression. These results suggested that activation of endogenous AMPK and the imbalance of mitochondrial homeostasis in the infarct area under acute stress were related to the inflammatory response in this area. Further analyses showed that compared with the vehicle group, myocardial AMPK-p/AMPK protein expression in the infarct area of the metformin group was down-regulated, the myocardial TSPO *in vivo* expression level decreased, and Bcl-2/Bax protein expression was up-regulated. These results suggested that metformin could maintain mitochondrial homeostasis and attenuate cardiomyocyte apoptosis by inhibiting endogenous myocardial AMPK activation in the infarct area before significant progression of LV remodelling.

At eight weeks after myocardial I/R injury, the *in vivo* TSPO expression level in cardiomyocytes in the distal non-infarcted area increased, no CD68$^+$ inflammatory cells were detected, and the expression levels of AMPK-p/AMPK and Bcl-2/Bax proteins decreased. These results suggested that mitochondrial homeostasis imbalance and cardiomyocyte apoptosis were still present in the area distal to the infarct at the late stage of heart failure, despite the lack of endogenous AMPK activation or CD68$^+$ cell accumulation in myocardial inflammatory cells in this area. Thackeray et al. [13] also reported no accumulation of CD68$^+$ cells in the high-TSPO expression area distal to the infarct at the late stage of

heart failure, which was speculated to be related to mitochondrial dysfunction. In the present study, metformin was used for intervention in myocardial I/R injury, which further decreased the uptake activity of ^{18}F-FDPA, and the expression of AMPK-p/AMPK and Bcl-2/Bax proteins increased in parallel. These results further confirmed the protective effects of metformin on mitochondrial function in the distal non-infarct area.

Systemic oxidative stress has been shown to affect the degree of repair of the damaged myocardium via paracrine action. Following myocardial infarction, the myocardium in the distal non-infarct area repairs the myocardial structure via the paracrine pathway, limiting LV expansion and protecting LV function [33]. Consistently, we found that compared with the vehicle group, the LVESV decreased and the LVEF increased in the metformin group, although there was no significant difference between the two groups. This finding suggests that the protective effects of metformin against myocardial injury at the late stage of heart failure might be related to changes in the microenvironment in the distal non-infarct area, which then activate AMPK through the paracrine pathway, improving myocardial cell viability in this area and limiting LV dilatation, ultimately protecting LV function. In the present study, we utilized gated PET/CT imaging to serially evaluate the changes of LV remodelling and the LVEF. Using this modality, we demonstrated that metformin therapy significantly improved LV function and inhibited LV remodelling, as evidenced by the increased LVEF and decreases in the LVESV compared with those of the vehicle group.

Our results also suggested that ^{18}F-FDPA PET imaging in chronic heart failure can provide a surrogate measure of mitochondrial homeostasis, which may be helpful for predicting LV remodelling and assessing the response to heart failure therapies. However, TSPO tracer uptake by the mitochondria-rich myocardial tissue could impact the resolution of inflammation against non-inflammatory signals in the early stage of I/R injury. Therefore, additional studies are needed to investigate the clinical implications of our findings.

In summary, this study is the first to demonstrate that prolonged administration of metformin exerted a pleiotropic protective effect against myocardial I/R injury, which was associated with a temporal and regional dynamic balance between mitochondrial homeostasis and cell death, as assessed by TSPO-targeted imaging during cardiac remodelling. Specifically, metformin attenuated the apoptosis of defected cardiomyocytes via an endogenous pathway at the early phase of I/R injury. Subsequently, prolonged treatment of metformin promoted mitochondrial homeostasis of remote cardiomyocytes at the chronic phase following I/R.

Declarations

Funding

This work was supported by the National Natural Science Foundation of China (grant numbers 81871377, 81571717).

Competing interests

The authors have no relevant financial or non-financial interests to disclose.

Authors' contributions

Jing Tian and Xiaoli Zhang designed the study. Tiantian Mou carried out the radiolabelling experiments. Yi Tian, Jing Tian, and YaQi Zheng performed the animal experiments. Jing Tian, Xiang Li, and Mingkai Yun interpreted and analysed the scans. Jing Tian analysed and interpreted the data. Jing Tian wrote the first draft of manuscript, which was revised by Marcus Hacker, Xiaoli Zhang, and Xiang Li. All authors read and approved the final manuscript.

Ethics approval

All animal experiments were performed according to Beijing's laboratory animal management regulations, and were approved by the Animal Care Committee of Capital Medical University (Ethical approval number: AEEI-2019-167).

Consent to participate

Not applicable.

Consent to publish

Not applicable.

References

1. Higuchi T, Fukushima K, Xia J, Mathews WB, Lautamaki R, Bravo PE, et al. Radionuclide imaging of angiotensin II type 1 receptor upregulation after myocardial ischemia-reperfusion injury. J Nucl Med. 2010;51:1956–61. doi:10.2967/jnumed.110.079855.
2. Kloner RA. Stunned and Hibernating Myocardium: Where Are We Nearly 4 Decades Later? J Am Heart Assoc. 2020;9:e015502. doi:10.1161/JAHA.119.015502.
3. Bertero E, Maack C. Metabolic remodelling in heart failure. Nat Rev Cardiol. 2018;15:457–70. doi:10.1038/s41569-018-0044-6.
4. Meng Y, Tian M, Yin S, Lai S, Zhou Y, Chen J, et al. Downregulation of TSPO expression inhibits oxidative stress and maintains mitochondrial homeostasis in cardiomyocytes subjected to anoxia/reoxygenation injury. Biomed Pharmacother. 2020;121:109588. doi:10.1016/j.biopha.2019.109588.
5. Lu LQ, Tian J, Luo XJ, Peng J. Targeting the pathways of regulated necrosis: a potential strategy for alleviation of cardio-cerebrovascular injury. Cell Mol Life Sci. 2021;78:63–78. doi:10.1007/s00018-020-03587-8.
6. Salameh A, Dhein S, Mewes M, Sigusch S, Kiefer P, Vollroth M, et al. Anti-oxidative or anti-inflammatory additives reduce ischemia/reperfusions injury in an animal model of cardiopulmonary

bypass. Saudi J Biol Sci. 2020;27:18–29. doi:10.1016/j.sjbs.2019.04.003.

7. Hardie DG. Role of AMP-activated protein kinase in the metabolic syndrome and in heart disease. FEBS Lett. 2008;582:81–9. doi:10.1016/j.febslet.2007.11.018.
8. Morrison A, Li J. PPAR-gamma and AMPK–advantageous targets for myocardial ischemia/reperfusion therapy. Biochem Pharmacol. 2011;82:195–200. doi:10.1016/j.bcp.2011.04.004.
9. Herzig S, Shaw RJ. AMPK: guardian of metabolism and mitochondrial homeostasis. Nat Rev Mol Cell Biol. 2018;19:121–35. doi:10.1038/nrm.2017.95.
10. Chen X, Li X, Zhang W, He J, Xu B, Lei B, et al. Activation of AMPK inhibits inflammatory response during hypoxia and reoxygenation through modulating JNK-mediated NF-kappaB pathway. Metabolism. 2018;83:256–70. doi:10.1016/j.metabol.2018.03.004.
11. Taliani S, Pugliesi I, Da Settimo F. Structural requirements to obtain highly potent and selective 18 kDa Translocator Protein (TSPO) Ligands. Curr Top Med Chem. 2011;11:860–86. doi:10.2174/156802611795165142.
12. Gavish M, Veenman L. Regulation of Mitochondrial, Cellular, and Organismal Functions by TSPO. Adv Pharmacol. 2018;82:103–36. doi:10.1016/bs.apha.2017.09.004.
13. Thackeray JT, Hupe HC, Wang Y, Bankstahl JP, Berding G, Ross TL, et al. Myocardial Inflammation Predicts Remodeling and Neuroinflammation After Myocardial Infarction. J Am Coll Cardiol. 2018;71:263–75. doi:10.1016/j.jacc.2017.11.024.
14. Rupprecht R, Papadopoulos V, Rammes G, Baghai TC, Fan J, Akula N, et al. Translocator protein (18 kDa) (TSPO) as a therapeutic target for neurological and psychiatric disorders. Nat Rev Drug Discov. 2010;9:971–88. doi:10.1038/nrd3295.
15. Mou T, Tian J, Tian Y, Yun M, Li J, Dong W, et al. Automated synthesis and preliminary evaluation of [(18)F]FDPA for cardiac inflammation imaging in rats after myocardial infarction. Sci Rep. 2020;10:18685. doi:10.1038/s41598-020-75705-2.
16. Vakeva AP, Agah A, Rollins SA, Matis LA, Li L, Stahl GL. Myocardial infarction and apoptosis after myocardial ischemia and reperfusion: role of the terminal complement components and inhibition by anti-C5 therapy. Circulation. 1998;97:2259–67. doi:10.1161/01.cir.97.22.2259.
17. Botker HE, Hausenloy D, Andreadou I, Antonucci S, Boengler K, Davidson SM, et al. Practical guidelines for rigor and reproducibility in preclinical and clinical studies on cardioprotection. Basic Res Cardiol. 2018;113:39. doi:10.1007/s00395-018-0696-8.
18. Kurhaluk N, Bojkova B, Radkowski M, Zaitseva OV, Kyriienko S, Demkow U, et al. Melatonin and Metformin Diminish Oxidative Stress in Heart Tissue in a Rat Model of High Fat Diet and Mammary Carcinogenesis. Adv Exp Med Biol. 2018;1047:7–19. doi:10.1007/5584_2017_128.
19. Karam HM, Radwan RR. Metformin modulates cardiac endothelial dysfunction, oxidative stress and inflammation in irradiated rats: A new perspective of an antidiabetic drug. Clin Exp Pharmacol Physiol. 2019;46:1124–32. doi:10.1111/1440-1681.13148.

20. Zhang X, Liu XJ, Hu S, Schindler TH, Tian Y, He ZX, et al. Long-term survival of patients with viable and nonviable aneurysms assessed by 99mTc-MIBI SPECT and 18F-FDG PET: a comparative study of medical and surgical treatment. J Nucl Med. 2008;49:1288–98. doi:10.2967/jnumed.107.046730.
21. Yun M, Nie B, Wen W, Zhu Z, Liu H, Nie S, et al. Assessment of cerebral glucose metabolism in patients with heart failure by (18)F-FDG PET/CT imaging. J Nucl Cardiol. 2020. doi:10.1007/s12350-020-02258-2.
22. Werner RA, Maya Y, Rischpler C, Javadi MS, Fukushima K, Lapa C, et al. Sympathetic nerve damage and restoration after ischemia-reperfusion injury as assessed by (11)C-hydroxyephedrine. Eur J Nucl Med Mol Imaging. 2016;43:312–8. doi:10.1007/s00259-015-3171-x.
23. Dorbala S, Ananthasubramaniam K, Armstrong IS, Chareonthaitawee P, DePuey EG, Einstein AJ, et al. Single Photon Emission Computed Tomography (SPECT) Myocardial Perfusion Imaging Guidelines: Instrumentation, Acquisition, Processing, and Interpretation. J Nucl Cardiol. 2018;25:1784–846. doi:10.1007/s12350-018-1283-y.
24. Autio A, Uotila S, Kiugel M, Kyto V, Liljenback H, Kudomi N, et al. (68)Ga-DOTA chelate, a novel imaging agent for assessment of myocardial perfusion and infarction detection in a rodent model. J Nucl Cardiol. 2020;27:891–8. doi:10.1007/s12350-019-01752-6.
25. Thackeray JT, Bankstahl JP, Wang Y, Wollert KC, Bengel FM. Targeting Amino Acid Metabolism for Molecular Imaging of Inflammation Early After Myocardial Infarction. Theranostics. 2016;6:1768–79. doi:10.7150/thno.15929.
26. Wang Y, Yang Z, Zheng G, Yu L, Yin Y, Mu N, et al. Metformin promotes autophagy in ischemia/reperfusion myocardium via cytoplasmic AMPKalpha1 and nuclear AMPKalpha2 pathways. Life Sci. 2019;225:64–71. doi:10.1016/j.lfs.2019.04.002.
27. Cadenas S. ROS and redox signaling in myocardial ischemia-reperfusion injury and cardioprotection. Free Radic Biol Med. 2018;117:76–89. doi:10.1016/j.freeradbiomed.2018.01.024.
28. Wang X, Yang L, Kang L, Li J, Yang L, Zhang J, et al. Metformin attenuates myocardial ischemia-reperfusion injury via up-regulation of antioxidant enzymes. PLoS ONE. 2017;12:e0182777. doi:10.1371/journal.pone.0182777.
29. Wu S, Zou MH. AMPK. Mitochondrial Function, and Cardiovascular Disease. Int J Mol Sci. 2020;21. doi:10.3390/ijms21144987.
30. Qi D, Young LH. AMPK: energy sensor and survival mechanism in the ischemic heart. Trends Endocrinol Metab. 2015;26:422–9. doi:10.1016/j.tem.2015.05.010.
31. Miller EJ, Li J, Leng L, McDonald C, Atsumi T, Bucala R, et al. Macrophage migration inhibitory factor stimulates AMP-activated protein kinase in the ischaemic heart. Nature. 2008;451:578–82. doi:10.1038/nature06504.
32. de Haan JJ, Smeets MB, Pasterkamp G, Arslan F. Danger signals in the initiation of the inflammatory response after myocardial infarction. Mediators Inflamm. 2013;2013:206039. doi:10.1155/2013/206039.

33. Farahmand P, Lai TY, Weisel RD, Fazel S, Yau T, Menasche P, et al. Skeletal myoblasts preserve remote matrix architecture and global function when implanted early or late after coronary ligation into infarcted or remote myocardium. Circulation. 2008;118:130-7. doi:10.1161/CIRCULATIONAHA.107.757617.

Figures

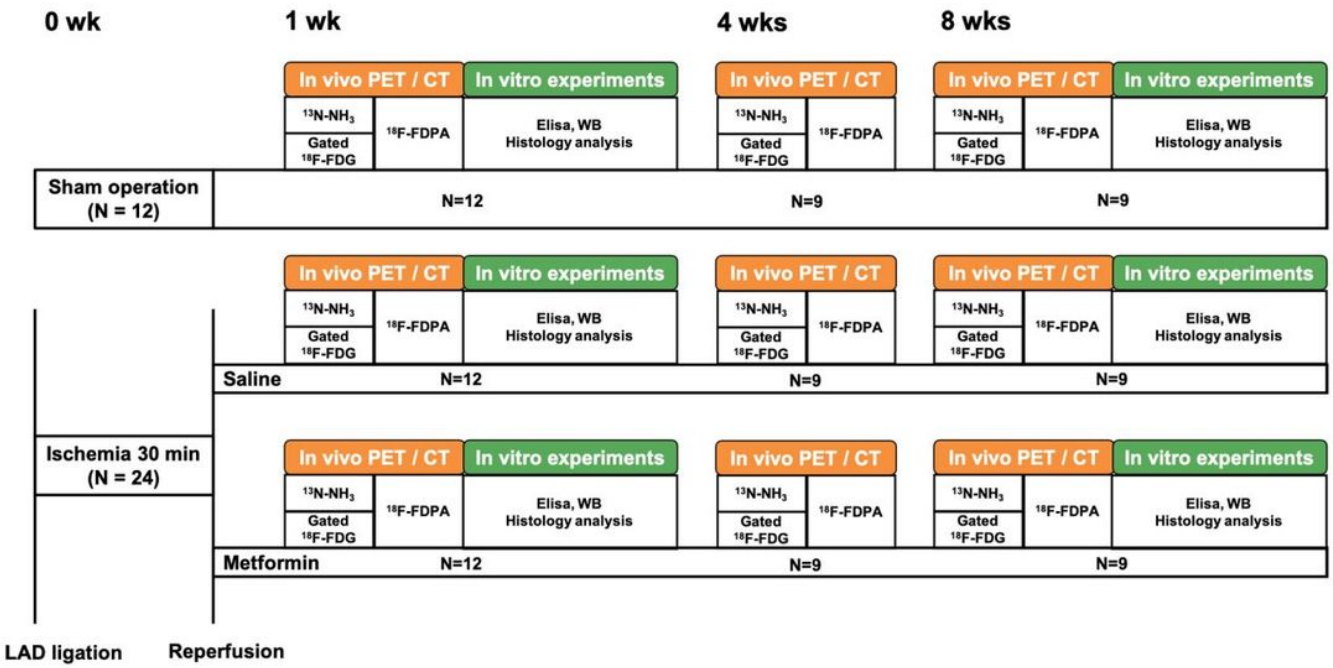

Figure 1

Flow diagram of experimental procedures in SD rats. Male SD rats (N = 36) were divided into the sham (n = 12) and myocardial I/R injury groups (n = 24). The I/R group was further divided into the vehicle (n = 12) and metformin (n = 12) groups. *In vivo* PET/CT and *in vitro* experiments analysis were performed on all rats. SD, Sprague-Dawley; I/R, ischemia-reperfusion; PET/CT, positron emission tomography/computed tomography; vehicle group: 0.9% saline; Elisa, enzyme-linked immunosorbent assay; WB, western blotting; LAD, left anterior descending artery.

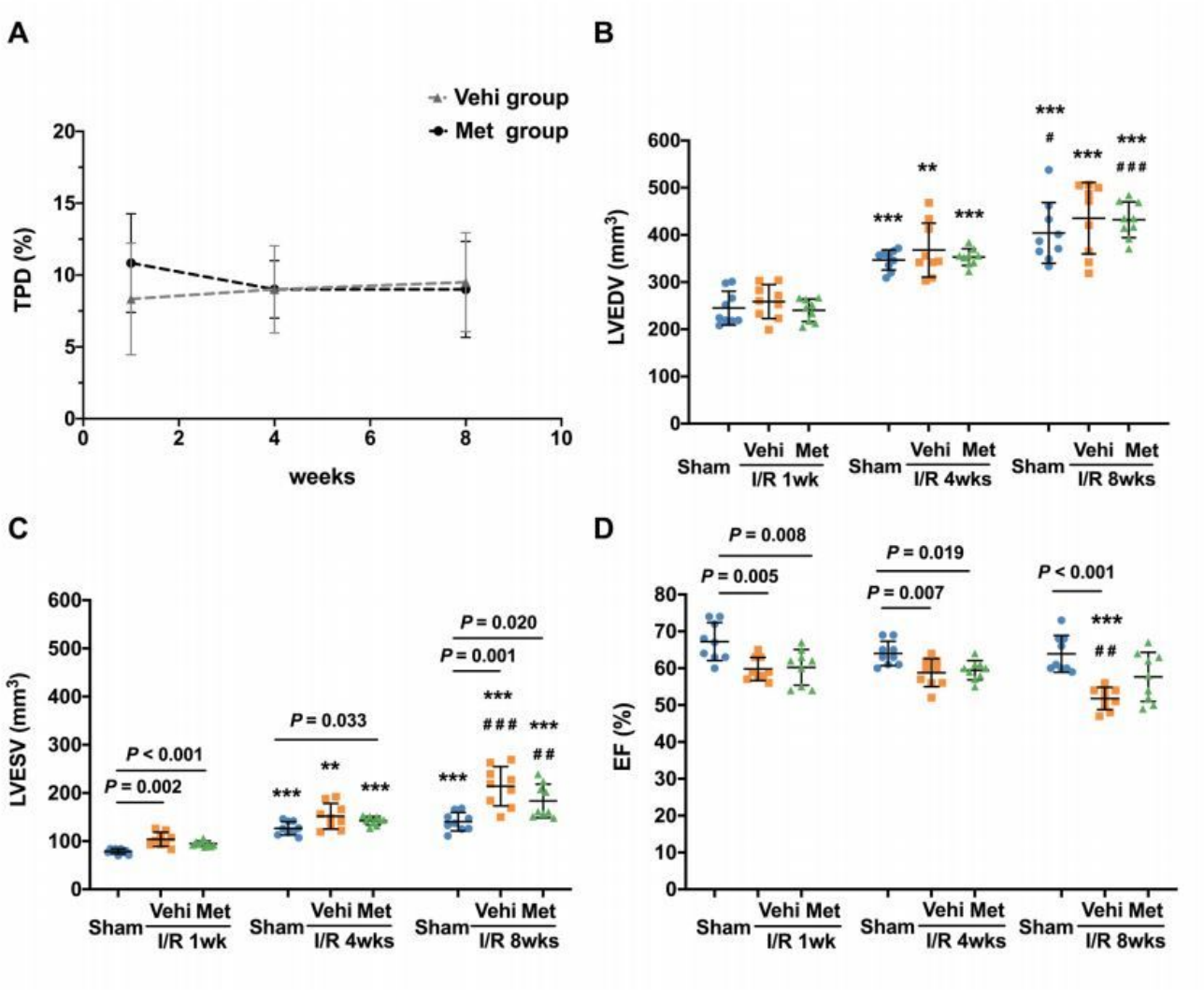

Figure 2

Anti-remodelling effects of metformin therapy on the rat heart after myocardial ischemia-reperfusion (I/R) injury. (a)^{13}N-NH_3 perfusion PET/CT was performed to determine the extent of the total perfusion defect (TPD) after I/R injury (Mann Whitney *U* test). Gated ^{18}F-FDG PET/CT revealed a significantly higher (b) left ventricular end-diastolic volume (LVEDV) and (c) left ventricular end-systolic volume (LVESV) after I/R injury when compared with those of the sham group, (d) leading to a significantly impaired left ventricular ejection fraction (LVEF), which was improved by metformin treatment over 8 weeks. N = 9 independent experiments. Vehi, saline; Met, metformin. Data are presented as a box plot (box, 25–75% interquartile range; centre line, median) overlaid with a dot plot (individual data points). $^{**}P < 0.01$, $^{***}P < 0.001$ *vs.* I/R 1wk; $^{\#}P < 0.05$, $^{\#\#}P < 0.01$, and $^{\#\#\#}P < 0.001$ *vs.* I/R 4wks (analysis of variance with Tukey's post-hoc tests)

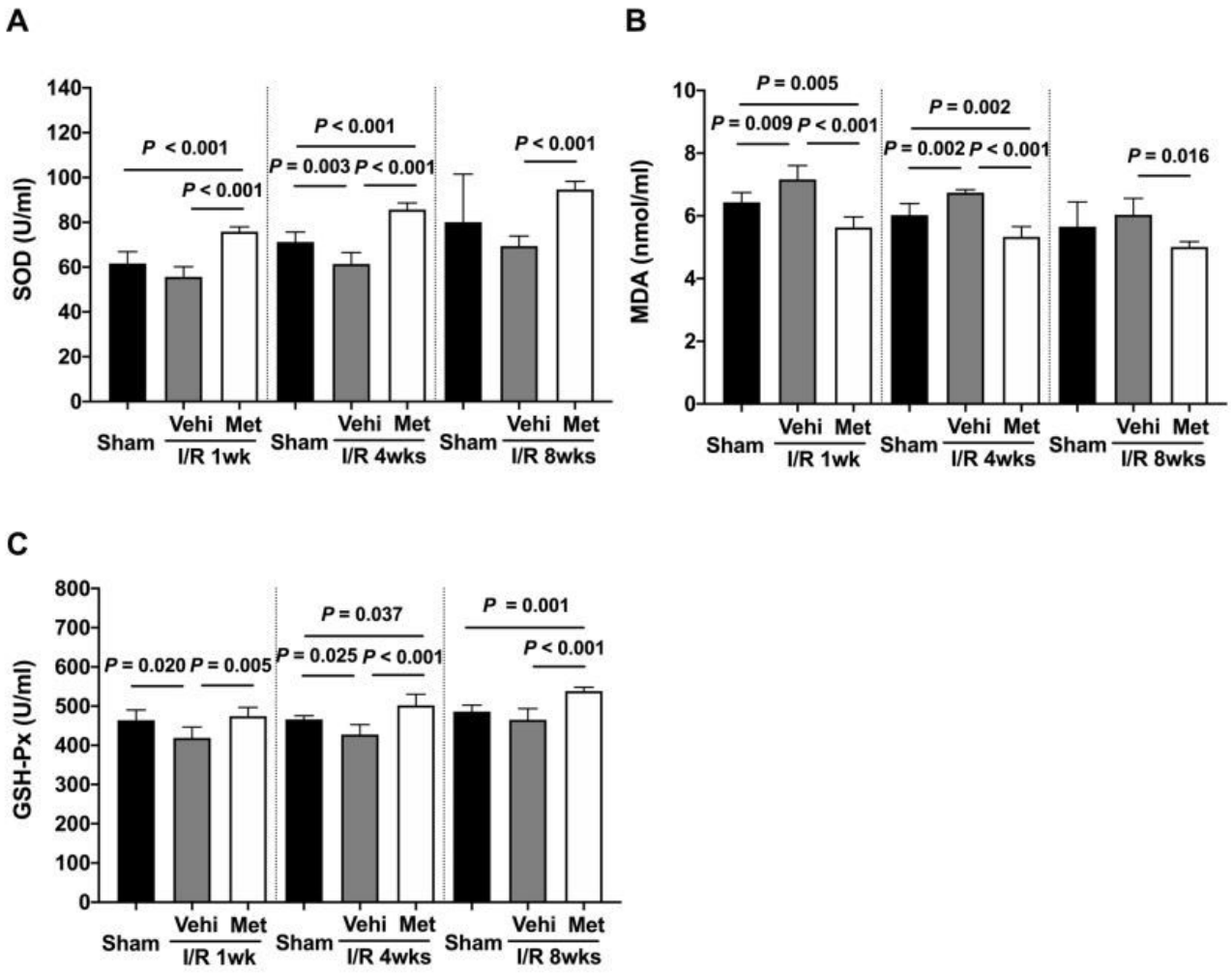

Figure 3

Anti-oxidative stress effect of metformin therapy after myocardial ischemia-reperfusion (I/R) injury. Serum levels of the anti-oxidative stress markers (a) SOD and (c) GSH-Px, and the oxidative stress marker (b) MDA in the three groups. N = 6 independent experiments. SOD, superoxide dismutase; MDA, malondialdehyde; GSH-Px, glutathione peroxidase; Vehi, saline; Met, metformin. Analysis of variance with Tukey's post-hoc tests

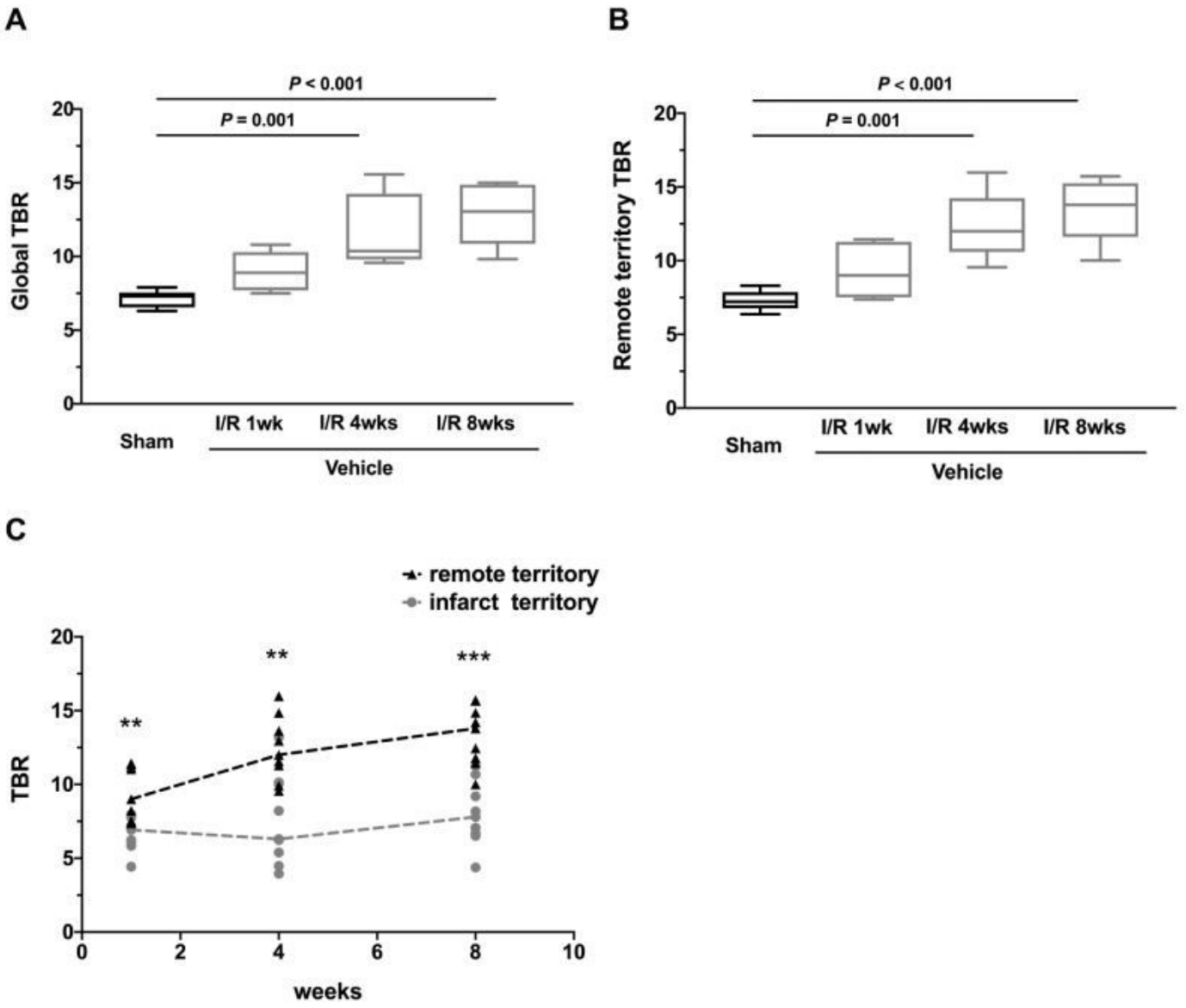

Figure 4

Mitochondrial dysfunction after myocardial ischemia-reperfusion (I/R) injury. Semi-quantitative analysis of the TSPO signal in the global (a) and remote (b) regions of the three groups over 8 weeks following I/R injury (or sham surgery). Data were analysed by the Kruskal-Wallis test with Dunn's post-hoc test.
The line graph (c) shows the time course of TSPO uptake activity in the remote (blue) and infarct (red) regions after myocardial I/R injury. Global target-to-background ratio (TBR) = the global SUVmean/LA SUVmean. Regional TBR = the regional SUVmean/LA SUVmean. N = 9 independent experiments. LA, left atrium; vehicle, saline. Data are presented as a box plot (box, 25–75% interquartile range; centre line, median) overlaid with a dot plot (individual data points). $^{**}P < 0.01$, $^{***}P < 0.001$ (Mann Whitney *U* test)

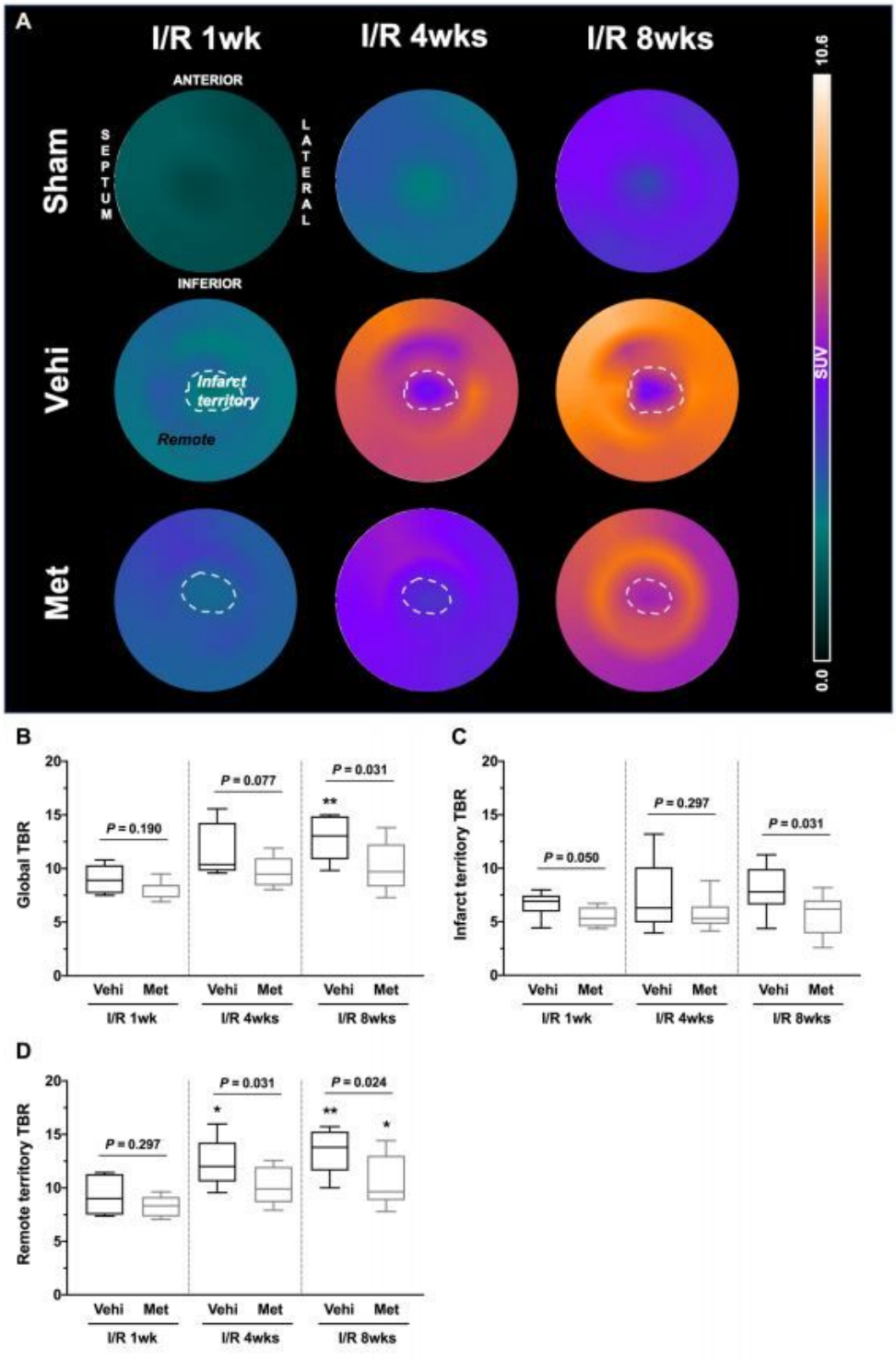

Figure 5

Metformin maintains mitochondrial homeostasis after myocardial ischemia-reperfusion (I/R) injury. Representative TSPO polar maps of the three groups over 8 weeks following I/R injury (a). The TSPO signal is shown for the sham group (top row), vehicle group (middle row), and metformin group (bottom row) at 1, 4, and 8 weeks after I/R injury. All serial images are scaled identically. Semi-quantitative analysis of the TSPO signal in the global (b), infarct territory (c), and remote non-infarct territory (d) of I/R

in the three groups over 8 weeks following I/R injury (or sham surgery). Global target-to-background ratio (TBR) = the global SUVmean/LA SUVmean. Regional TBR = the regional SUVmean/LA SUVmean. N = 9 independent experiments. LA, left atrium; Vehi, saline; Met, metformin. Data are presented as a box plot (box, 25–75% interquartile range; centre line, median) overlaid with a dot plot (individual data points). $^{*}P<0.05$, $^{**}P<0.01$ *vs.* I/R 1wk (Mann Whitney *U* test and Kruskal-Wallis test with Dunn's post-hoc test)

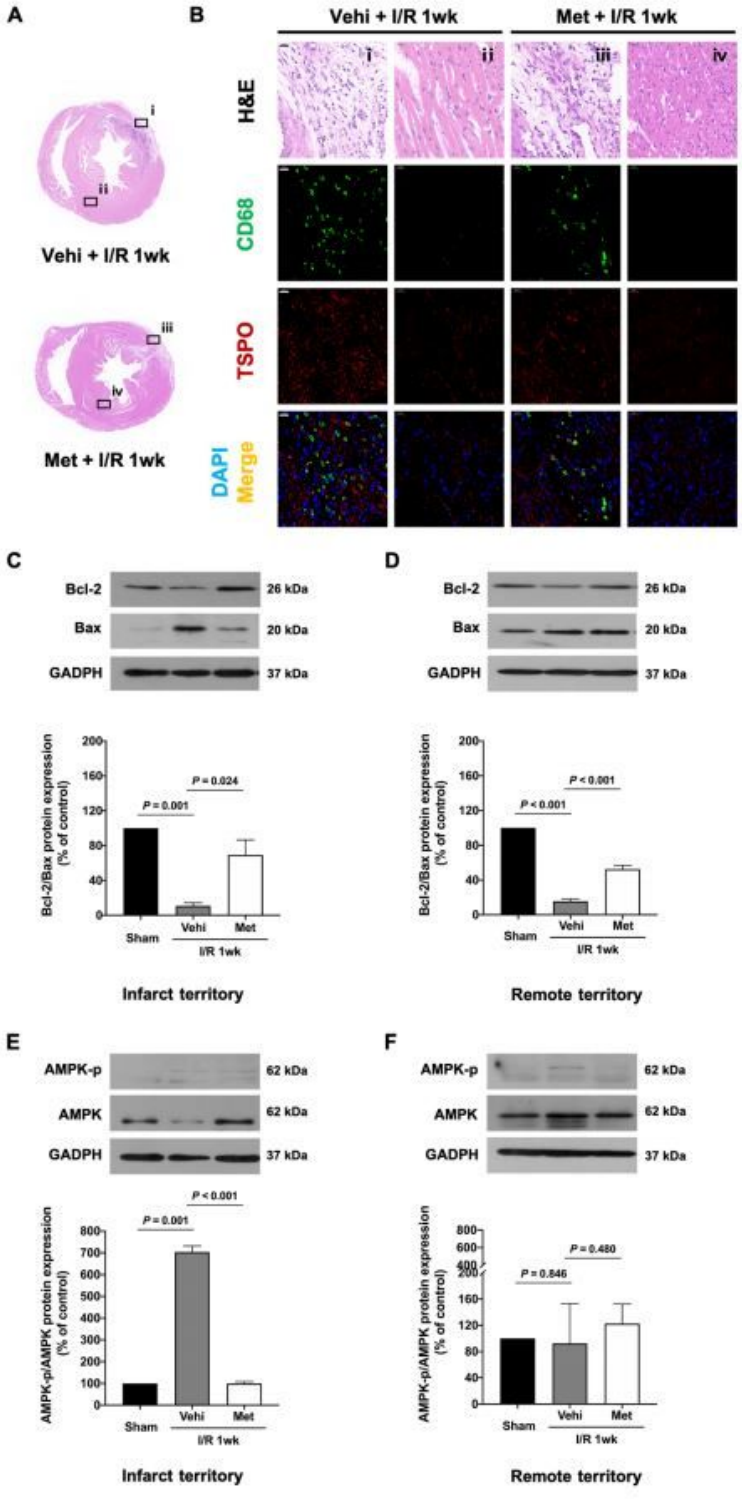

Figure 6

Metformin protects against ischemia-reperfusion (I/R)-induced mitochondrial dysfunction and apoptosis by inhibiting endogenous AMPK in the infarct territory at acute phase. (a) Haematoxylin and eosin (H&E) staining to define the general myocardial morphology and local position for the acute infarct territory (i, iii) and remote territory (ii, iv) in the vehicle and metformin groups at 1 week after I/R injury. (b) Gross histological sections stained with H&E indicating the position of inflammation under a light microscope (magnification 40×, scale bar = 20 mm) (top row). Confocal fluorescence microscopy with dual fluorescent staining for CD68 (green, second row) and TSPO (red, third row). Blue fluorescence of diamidine-phenylindole (DAPI) identifies the nuclei in the fused images (bottom row). Western blot analysis and quantification for apoptosis-related proteins Bcl-2/Bax in the infarct territory (c) and remote territory (d) (N = 3 per group). Western blot analysis and quantification of AMPK pathway-related proteins AMPK-p/AMPK in the infarct territory (e) and remote territory (f) (N = 3 per group). Vehi, saline; Met, metformin. *P* values are based on the Student t-test

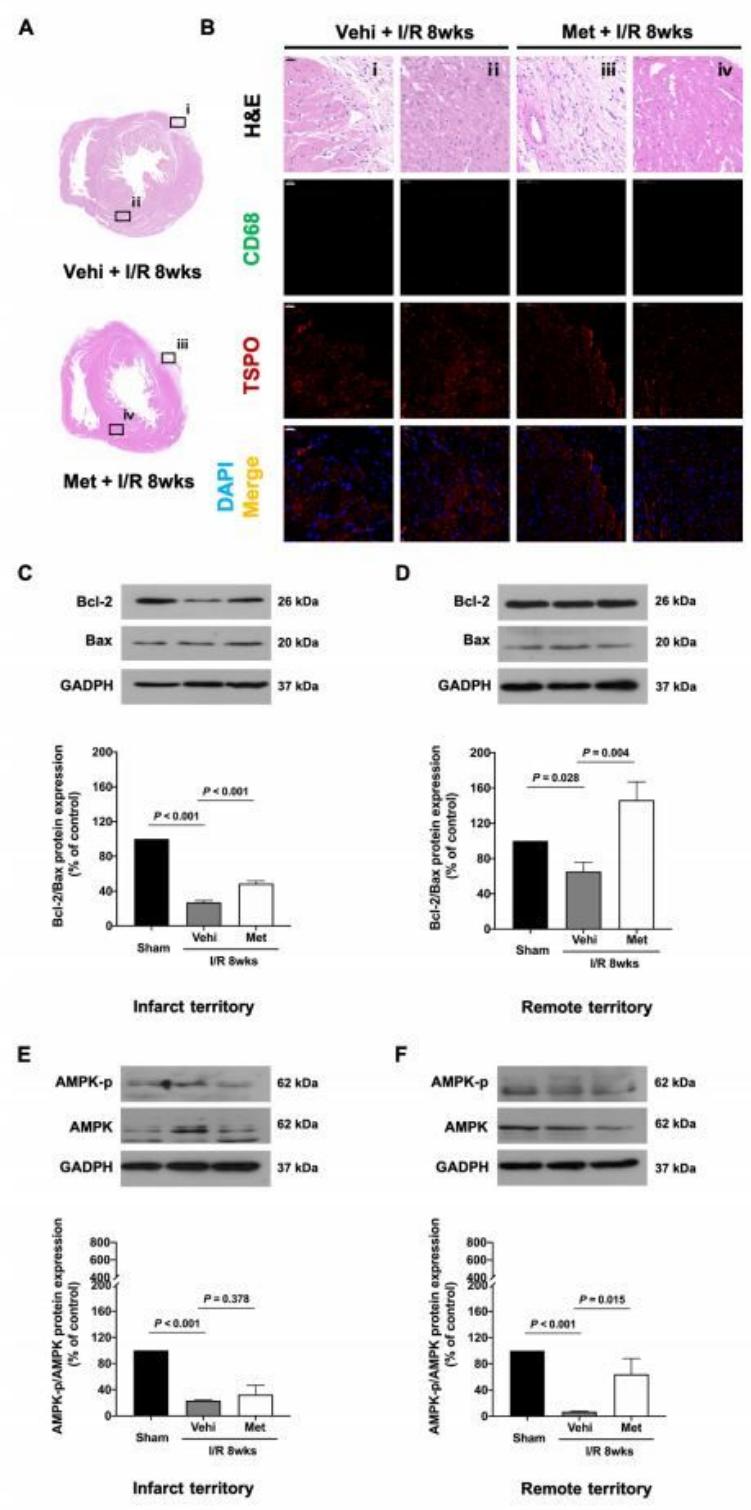

Figure 7

Metformin protects against ischemia-reperfusion (I/R)-induced mitochondrial dysfunction and apoptosis by promoting exogenous AMPK in the remote territory at the chronic phase after injury (8 weeks). (a) Haematoxylin and eosin (H&E) staining to define the general myocardial morphology and local position for the chronic infarct territory (i, iii) and remote territory (ii, iv) in the vehicle and metformin groups at 8 weeks after I/R injury. (b) Gross histological sections stained with H&E indicating the positioning of

inflammation under a light microscope (magnification 40×, scale bar = 20 mm) (top row). Confocal fluorescence microscopy with dual fluorescent staining for the monocyte marker CD68 (green, second row) and the imaging target TSPO (red, third row). Blue fluorescence of diamidine-phenylindole (DAPI) identifies the nuclei in the fused images (bottom row). Western blot analysis and quantification for apoptosis-related proteins Bcl-2/Bax in the infarct territory (c) and remote territory (d) (N = 3 per group). Western blot analysis and quantification of AMPK pathway-related proteins AMPK-p/AMPK in the infarct territory (e) and remote territory (f) (N = 3 per group). Vehi, saline; Met, metformin. *P* values are based on the Student t-test